Molecular Biology of the Cell
Vol. 12, 3060–3073, October 2001

Characterization of Human Palladin, a Microfilament-associated Protein

Olli-Matti Mykkänen, Mikaela Grönholm, Mikko Rönty, Maciej Lalowski, Paula Salmikangas, Heli Suila, and Olli Carpén*

Department of Pathology, Helsinki University Hospital, and Neuroscience Program, Biomedicum, University of Helsinki, FIN-00014 Helsinki, Finland

Submitted August 10, 2000; Revised May 15, 2001; Accepted July 27, 2001
Monitoring Editor: Ted Salmon

Actin-containing microfilaments control cell shape, adhesion, and contraction. In striated muscle, α-actinin and other Z-disk proteins coordinate the organization and functions of actin filaments. In smooth muscle and nonmuscle cells, periodic structures termed dense bodies and dense regions, respectively, are thought to serve functions analogous to Z-discs. We describe here identification and characterization of human palladin, a protein expressed mainly in smooth muscle and nonmuscle and distributed along microfilaments in a periodic manner consistent with dense regions/bodies. Palladin contains three Ig-domains most homologous to the sarcomeric Z-disk protein myotilin. The N terminus includes an FPPPP motif recognized by the Ena-Vasp homology domain 1 domain in Ena/vasodilatator-stimulated phosphoprotein (VASP)/Wiscott-Aldrich syndrome protein (WASP) protein family. Cytoskeletal proteins with FPPPP motif target Ena/VASP/WASP proteins to sites of actin modulation. We identified palladin in a yeast two-hybrid search as an ezrin-associated protein. An interaction between palladin and ezrin was further verified by affinity precipitation and blot overlay assays. The interaction was mediated by the α-helical domain of ezrin and by Ig-domains 2–3 of palladin. Ezrin is typically a component of the cortical cytoskeleton, but in smooth muscle cells it is localized along microfilaments. These cells express palladin abundantly and thus palladin may be involved in the microfilament localization of ezrin. Palladin expression was up-regulated in differentiating dendritic cells (DCs), coinciding with major cytoskeletal and morphological alterations. In immature DCs, palladin localized in actin-containing podosomes and in mature DCs along actin filaments. The regulated expression and localization suggest a role for palladin in the assembly of DC cytoskeleton.

INTRODUCTION

Actin-containing microfilaments play an essential role in determining cell shape, and in cell locomotion and contractility. Filamentous actin and actin-associated proteins can assemble into higher order structures, such as filopodia, microspikes, lamellipodia, and stress fibers. In various cell types, microfilaments (termed thin filaments in skeletal muscle) interact with myosin and with other proteins to provide machinery for coordinated contraction.

In the contractile unit of the skeletal muscle, i.e., the sarcomere, the thin filaments are interconnected and aligned at specialized structures, the Z-discs (Fürst and Gautel, 1995; Young *et al.*, 1998). In smooth muscle, actin filaments emerge obliquely from structural elements termed dense bodies (reviewed by Small and Gimona, 1998; Stromer 1998). Thus, in smooth muscle, the dense bodies serve a function analogous to the Z-discs. Stress fibers are bundles of actin microfilaments linked to the cell membrane in specific cell attachment sites, focal adhesions. Stress fibers are present in most adherent cell types. They are also organized in a periodical manner and contain structural elements called dense regions (Katoh *et al.*, 1998). A common constituent of Z-discs, dense bodies, and the dense regions is α-actinin, an actin cross-linking protein involved in the arrangement of actin filaments (Geiger *et al.*, 1981; Langanger *et al.*, 1984; Chou *et al.*, 1994; Young *et al.*, 1998). Apart from α-actinin, several other components of the Z-disk have been identified (Fürst and Gautel, 1995; Young *et al.*, 1998), whereas the constituents of dense bodies and dense regions are still poorly characterized.

We recently identified a structural protein of the striated muscle Z-discs, myotilin, which contains a unique serine-rich N terminus and two Ig-like domains in its C terminus

* Corresponding author. E-mail address: olli.carpen@helsinki.fi.
Abbreviations used: DC, dendritic cell; ERM, ezrin/radixin/moesin; EVH1, Ena-Vasp homology domain 1; HISM, human intestinal smooth muscle; VASP, vasodilatator-stimulated phosphoprotein; WASP, Wiscott-Aldrich syndrome protein.

(Salmikangas *et al.*, 1999). Myotilin interacts with α-actinin (Salmikangas *et al.*, 1999) and γ-filamin (van der Ven *et al.*, 2000), and a missense mutation in myotilin gene is associated with limb-girdle muscular dystrophy 1A (Hauser *et al.*, 2000). In this work we report identification of a structurally related molecule that is expressed in epithelial and mesenchymal cells, including smooth muscle, but only weakly in skeletal muscle. The protein was discovered in a yeast two-hybrid screen with the use of the ezrin/radixin/moesin (ERM) family member, ezrin, as bait. During characterization of this novel human protein, the mouse ortholog, termed palladin, was identified with the use of a different approach, which was based on the immunoreactivity of an antibody that recognized a novel component of the actin cytoskeleton (Parast and Otey, 2000). Palladin and myotilin are homologous both in their unique N-terminal regions and in the C-terminal Ig-domains but, unlike myotilin, palladin contains additional polyproline stretches, which include an FPPPP motif implicated in regulation of actin assembly. Subcellular localization along microfilaments in a punctate manner indicates that palladin is a component of the actin cytoskeleton.

MATERIALS AND METHODS

cDNA Cloning of Human Palladin and Sequence Analysis

The yeast two-hybrid technique used for library screening has been described (Gyuris *et al.*, 1993). A C-terminal cDNA construct encoding amino acids 278–585 of human ezrin was subcloned into the EG202 bait vector. A HeLa cell cDNA library in JG4-5 prey vector was transformed into 10^6 yeast cells expressing the ezrin bait. The cells were plated as replicates on agarose plates supplemented with the appropriate amino acids, and either glucose or galactose, the latter for the induction of the library inserts. Clones producing β-galactosidase were isolated, and the cDNAs were purified and sequenced.

An 899-bp cDNA clone from the yeast two-hybrid analysis was used as a probe to screen human λDR2 fetal liver, λDR2 fetal placenta, and λgt11 small intestine libraries (all from CLONTECH, Palo Alto, CA) according to manufacturer's protocol. Additional sequence information was also obtained from BLAST database (http://www.ncbi.nlm.nih.gov/BLAST). Domain prediction was performed with Pfam sequence alignment tool (http://www.sanger.ac.uk/Software/Pfam/search.shtml). Sequence alignment and the phylogeny analysis of Ig-domain containing cytoskeletal proteins were compiled with Megalign software (DNASTAR) with the use of Clustal-W algorithm.

Northern Blot Analysis

Northern blot analysis was performed with a commercial multiple tissue mRNA filter (CLONTECH). A ^{32}P-labeled 610-bp probe was polymerase chain reaction-amplified with forward primer 5′-ACCTGCTCCCTCCATACCACAGC and reverse primer 5′-CTCCCAATACACGACATTCCAGCC. The hybridization was carried out according to manufacturer's instructions.

Cell Cultures and Transfections

HeLa (American Type Culture Collection, Manassas, VA) and U251 mg of malignant glioma cells (Westermark *et al.*, 1973) were grown in modified Eagle's medium supplemented with 10% fetal calf serum. Human intestinal smooth muscle cells (HISMs; American Type Culture Collection) were grown in modified Eagle's medium supplemented with 15% fetal calf serum and 2% Ultroser-G (Invitrogen, Carlsbad, CA). For transient expression, the C-terminal coding region of palladin was polymerase chain reaction-amplified with primers 5′-CCTGTGGAATTCATGGCACCATTCTTTGAGAT and 5′-TGGTCAAGGCAATGGCTGTTT, with the use of clone AB023209 as the template (gift of Dr. Takahiro Nagase, Kazusa DNA Research Institute, Kazusa, Japan) (Nagase *et al.*, 1999). The product was subcloned into the *Eco*RI site of myc-tagged pCI-neo vector (Promega, Madison, WI). The authenticity of the construct was verified by sequencing. HeLa cells were transfected with the use of FuGENE 6 (Boehringer Mannheim, Mannheim, Germany) transfection reagent. After 48 h the cells were washed twice, fixed with 3.5% paraformaldehyde (PFA), and used for immunolocalization.

Dendritic cells (DCs) were obtained as follows. Peripheral blood monocytes were isolated from heparinized blood of healthy donors by Ficoll-Paque (Amersham Pharmacia Biotech AB, Uppsala, Sweden) centrifugation followed by Percoll (Amersham Pharmacia Biotech AB) gradient centrifugation. Adherent monocytes were used after purification or differentiated into immature DCs for 7 d in RPMI-1640 supplemented with 10% fetal bovine serum (Invitrogen), 25 ng of interleukin-4 (Endogen, Rockford, IL), and 100 ng/ml GM-CSF (granulocyte macrophage colony stimulating factor) (Schering-Plough, Kenilworth, NJ) (Romani *et al.*, 1994; Sallusto and Lanzavecchia, 1994). Mature DCs were achieved by 24-h incubation with 5 μg/ml lipopolysaccharide from *Escherichia coli* serotype 026:B6 (Sigma, St. Louis, MO). Cells were labeled with fluorescein isothiocyanate (FITC)-antihuman-CD83, FITC-anti-human-CD1a (BD PharMingen, San Diego, CA), or FITC-IgG1 control antibody (BD Biosciences, Franklin Lakes, NJ), and analyzed by FACScan flow cytometer.

Antibody Production and Western Blotting

A polyclonal antibody was increased in rabbits with the use of a synthetic branched lysine core peptide (QEPEEETANQEYKVSSC, amino acids 337–353; Figure 1A) as an antigen. After six immunizations, rabbits were bled. The immunoreactive antibody fraction affinity purified in a glutathione *S*-transferase (GST)-palladin column (amino acids 321–772). The specificity of the antiserum was tested by comparing the reactivity against the recombinant GST-palladin and an irrelevant GST-fusion protein (GST-cdk2, kindly provided by Dr. Tomi Mäkelä, University of Helsinki, Helsinki, Finland) in Western blotting. Blocking experiments, in which the antibody was preabsorbed with 5 M excess of the antigenic or irrelevant control peptide, were also performed.

For Western blotting, confluent 10-cm plates of HISM, U251mg, and HeLa cells or equal amounts of various tissues were lysed in Laemmli buffer. Monocytes, and immature and mature DCs were lysed in ice cold ELB lysis buffer (50 mM HEPES, pH 7.4, 150 mM NaCl, 5 mM EDTA, 1% NP-40) supplemented with protease inhibitors, the protein concentrations were equalized with the use of Protein assay reagent (Bio-Rad, Hercules, CA), and equal amounts of protein were boiled in Laemmli buffer. Lysates were resolved in 8 or 10% SDS-PAGE, and transferred onto nitrocellulose filters. The filters were probed with palladin antibody or preimmune serum (1:1000 dilution), or with goat anti-moesin antibody (1:1500) (Santa Cruz Biotechnology, Santa Cruz, CA), followed by peroxidase-conjugated swine anti-rabbit or anti-goat IgG (DAKO, Copenhagen, Denmark), and detected by enhanced chemiluminescence (Pierce Chemical, Rockford, IL) or with the use of biotinylated goat-anti-rabbit antibody followed by avidin biotin complex-horseradish peroxidase (HRP) complex.

Immunofluorescence and Immunohistochemical Analysis

For immunofluorescence microscopy, cells grown on glass coverslips were fixed in 3.5% PFA (+4°C) for 5 min. The cells were permeabilized with 0.1% Triton X-100, and reacted with palladin

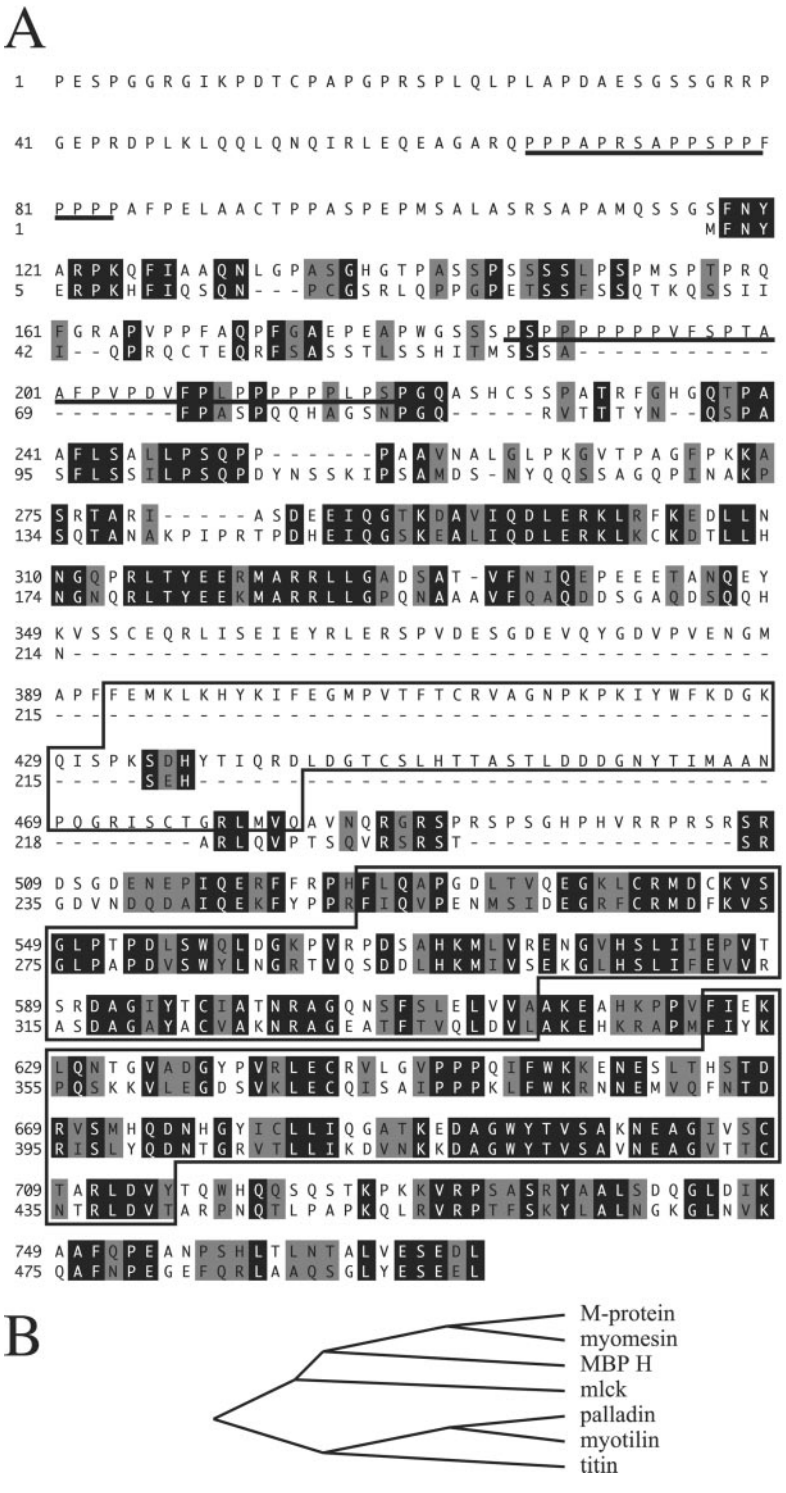

Figure 1. Amino acid sequence of human palladin and myotilin, and phylogeny of Ig-domain–containing proteins. (A) Amino acid sequence of human palladin (top sequence) in comparison with human myotilin is shown. Black boxes show identical residues and gray boxes conservative changes. The polyproline regions in palladin are underlined. The first polyproline region contains an FPPPP consensus sequence involved in binding to Ena/VASP/WASP family of proteins. The 3 Ig-domains are boxed. (B) Phylogeny tree of intracellular Ig-domain–containing proteins. The comparison was based on sequence alignment of Ig-domains only. MBP H, myosin binding protein H; mlck, myosin light chain kinase.

antibody or with preimmune serum, diluted at 1:100, followed by rhodamine-conjugated $F(ab)_2$ fragments of goat antirabbit antibody (Jackson Immunoresearch, West Grove, PA). For detection of transfected palladin, the anti-myc-tag mAb 7E12 (Babco, Berkeley, CA) was used at 1:500 dilution, followed by FITC-conjugated goat anti-mouse IgG (Cappel Research Products, Durham, NC). Ezrin was detected with monoclonal antibody (mAb) 3C12 (Böhling *et al.*, 1996) and F-actin with FITC-labeled phalloidin (Molecular Probes, Eugene, OR). DCs were grown on fibronectin-coated coverslips (5 h for monocytes, 24 h for immature DCs, 24 h in the presence of lipopolysaccharide for mature DCs). DCs, and HISM cells in some experiments, were briefly extracted (four times 5 s in 0.5% Triton

X-100, 75 mM KCl, 0.1 mM $MgCl_2$, 1 mM EGTA, 10 mM imidazole-HCl, pH 7.4) (Sainio *et al.*, 1997) and then fixed in 3.5% PFA (+4°C). After blocking Fc receptors with 2.4G2 antibody (American Type Culture Collection), DCs were stained as described above.

Human stomach tissue was embedded in Tissue-Tek (Sakura Finetek Europe, Zoeterwoude, The Netherlands), frozen in liquid nitrogen, and stored at −80°C. Six-micrometer frozen sections were immobilized on poly-L-lysine–coated glass slides and fixed in cooled acetone. For immunohistochemical staining, the sections were reacted with 1:250 dilution of palladin or preimmune serum. The antibody was detected with Elite Vectastain ABC kit (Vector Laboratories, Burlingame, CA). The slides were briefly counterstained with hematoxylin and eosin. All microscopy was performed on Zeiss Axiophot photomicroscope (Carl Zeiss, Oberkochen, Germany), and photographs were taken with a cooled charge-coupled device camera interfaced with analySIS 3.0 software (Soft Imaging System, Münster, Germany).

Yeast Two-Hybrid Analysis of Interaction between Human Palladin and Ezrin

To map the interaction domains, ezrin constructs 1–585 (wt), 1–339, and 479–585 were cloned into the EG202 bait vector, and palladin constructs Ig1–3, Ig1, and Ig2–3 were cloned into the JG4-5 prey vector. The constructs were transformed into BOY1-yeast of both α (kindly provided by P. Ljungdahl, Ludwig Institute for Cancer Research, Stockholm, Sweden) and **a** (Grönholm *et al.*, 1999) mating type. Baits and preys were grown on selection plates, replica plated together on rich media plates for mating overnight and replica plated on double (tryptophane and histidine) selection with 5-bromo-4-chloro-3-indolyl-β-D-galactopyranoside (Boehringer-Mannheim GmbH) for detection of interactions.

Affinity Precipitation Analysis

GST-ezrin 278–531, GST-ezrin 477–585, and GST in pGEX4T1 (Amersham Pharmacia Biotech AB) were expressed in *E. coli* DH5α cells and purified by glutathione-Sepharose beads as described (Turunen *et al.*, 1994). Yeast cells expressing an equal amount of hemagglutinin (HA)-tagged palladin constructs Ig1 and Ig2–3 and an ezrin construct containing the N-terminal domain (amino acids 1–309) were grown overnight in selective medium to an OD_{600} of 0.8–1.0. Cells were washed once with phosphate-buffered saline and lysed with a mini bead beater (BioSpec Products, Bartlesville, OK) in the presence of 1 ml of acid-washed glass beads (Sigma) in 200 μl of ELB buffer, 1% NP-40-buffer, and protease inhibitors. The debris was removed by centrifugation, and the supernatant diluted to a NP-40 concentration of 0.5%. Protein concentration was measured at A_{280} nm. Total protein (250 μg) was incubated with purified GST-fusion protein bound to glutathione-Sepharose beads (~1 μg) for 1 h. The beads were pelleted, the supernatant removed, and the beads washed in ELB-0.1% NP-40 buffer. Bound proteins were eluted from the beads by boiling in Laemmli buffer, separated in 10% SDS-PAGE gels, and analyzed by immunoblotting with the use of anti-HA antibody 12CA5 mAb (Boehringer Mannheim GmbH) at a dilution of 1:1500.

Blot Overlay Experiments

GST-palladin Ig2–3, GST-palladin Ig1–3, GST, and GST-ezrin 1–309 were expressed and purified as described above and GST-palladin Ig2–3, GST-palladin Ig1–3, GST were biotinylated (Gary and Bretscher, 1993). GST was cleaved of the ezrin 1–309 construct by thrombin. Full-length ezrin was purified as described (Heiska *et al.*, 1998). HISM and U251mg cells were lysed in ELB buffer, 1% NP-40, and protease inhibitors. Cell lysates, or purified wild-type or recombinant N-terminal ezrin 1–309 (1 μg/lane) were run in 10%SDS-PAGE, blotted onto nitrocellulose filters, and blocked overnight with the use of 3% bovine serum albumin in Tris-buffered saline-0.1% Tween 20. The blots were incubated with the biotinylated probe, GST, GST-palladin Ig2–3, and GST-palladin Ig1–3 (0.1 μg/ml) in 1% bovine serum albumin in Tris-buffered saline-0.1% Tween 20 for 2 h. HRP-conjugated extravidin (Sigma) (dilution 1:10.000) was detected with the use of enhanced chemiluminescence. The filters were stripped after each probe in 0.7% β-mercaptoethanol, 62.5 mM Tris pH 6.8, 2% SDS in 60°C for 20 min. The last immunoblotting was done with the rabbit ezrin antiserum BIII diluted 1:1000 (Turunen *et al.*, 1994).

RESULTS

Cloning and Sequence Analysis of Palladin cDNA

We searched for novel molecules interacting with ezrin with the use of a construct containing the α-helical and C-terminal domains (amino acids 278–585; see Figure 8 for the domain structure of ezrin) as bait in a yeast two-hybrid screen. With this approach, we identified from a HeLa cell library two identical 899-bp clones encoding for the last 254 amino acids (aa) of a novel gene product. Screening of human phage libraries yielded additional clones, the longest of which was 3655 bp. Additional sequence information was obtained from the BLAST database, which included the 4347-bp cDNA clone (accession no. AB023209, protein accession no. KIAA0992), predicted to encode the C-terminal 772 aa of a novel protein (Figure 1). Because the mouse ortholog was identified during the progress of this work (Parast and Otey, 2000), and termed palladin, we have decided to agree with the nomenclature, and term also the human protein palladin. It is possible that the clone AB023209 does not represent an entire coding region, because it does not contain an in frame stop codon or a Kozak consensus sequence before the first ATG codon.

Nonredundant database search revealed further sequence information, including two clones (accession no. AF077041 and accession no. AF151909), with minor nucleotide differences. Both clones contain the 3′-terminal sequence of palladin. Based on our sequencing results and comparisons with overlapping EST sequences, AF077041 contains the correct sequence. The 3865-bp cDNA contains a 647-bp 5′-untranslated sequence, an in-frame stop at nucleotide 594, an ATG codon at nucleotide 648 with a Kozak consensus sequence to initiate translation, a 1155-bp open reading frame that encodes a 385 aa polypeptide, and a 2-kb 3′-untranslated sequence. It is possible that this EST represents a short palladin isoform, however, this matter requires further investigation.

Comparison of the human amino acid sequence with the mouse ortholog (Parast and Otey, 2000) shows a divergence in the coding sequence within the very N-terminal sequence. The first 60 amino acids of mouse palladin are different from the 44 first residues of the human palladin sequence. Analysis of the most recent human genomic draft sequence (December 12, 2000 freeze) suggests that the site of cDNA divergence contains an exon-intron boundary in the human gene, and thus the N-terminal human and mouse sequences may represent differently spliced exons. After the short N-terminal diverging region, the sequence across these species is highly homologous, showing 89% identity ands 91% similarity (identical + conserved residues) within the last 728 residues (residues calculated from human sequence).

By structural prediction, human palladin contain three Ig-domains in the C-terminal part of the molecule. These

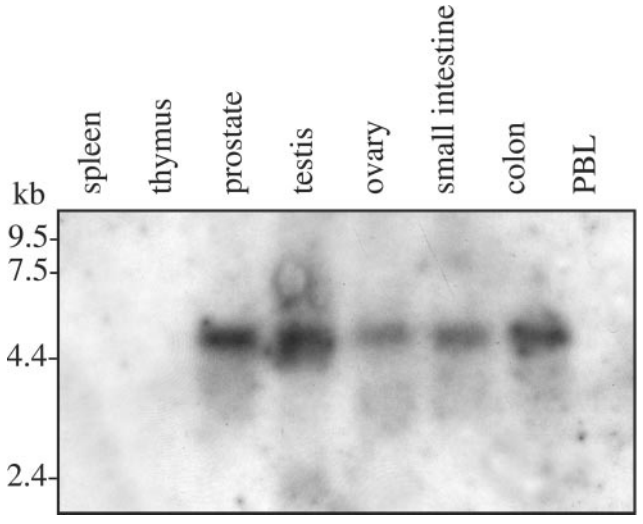

Figure 2. Northern blot analysis of palladin. A multiple tissue mRNA filter was hybridized with a ^{32}P-labeled 610-bp fragment of palladin cDNA. A major 4.5-kb transcript is detected in most tissues; however, hematopoetic organs and peripheral blood lymphocytes are negative.

Ig-domains are most homologous to those found in myotilin, a recently characterized Z-disk associated sarcomeric protein (49% identity with Ig-domains 2 and 3 of palladin). The Ig-domains of palladin are also homologous to Ig-domains Z6–8 present in the Z-disk associated region of the sarcomeric protein titin (31% identity). There is also homology to other cytoskeletal Ig-domain containing proteins. In Figure 1B, the comparison of the Ig-domain containing regions of several of these proteins is depicted as a phylogenetic tree. The result indicates that palladin is more related to myotilin and titin than to other Ig-domain–containing proteins.

The amino acid prediction is shown in Figure 1A. Part of the N-terminal region is homologous to myotilin (34% identity and 44% similarity for residues 118–327 of palladin and 2–191 of myotilin). However, palladin has two polyproline stretches not found in myotilin. The first stretch contains proline-rich consensus motif FPPPP that is recognized by the Ena-Vasp homology domain 1 (EVH1) found in Ena/vasodilatator-stimulated phosphoprotein (VASP)/Wiscott-Aldrich syndrome protein (WASP) family of proteins that control spatial actin assembly (Niebuhr *et al*., 1997).

Expression Pattern of Palladin

Northern blot analysis indicated that palladin mRNA transcript is present in a wide variety of tissues (Figure 2). A strong signal was seen in prostate, testis, ovary, small intestine, and colon. Weaker or nondetectable signal was present in hematopoietic tissues: thymus, spleen, and peripheral blood lymphocytes. The size of the major transcript was ~4.5 kb.

A rabbit antiserum was raised against a 17-residue synthetic peptide encompassing a region N-terminal to the first Ig-domain, and affinity purified in a GST-palladin column. The palladin antibody specifically recognized recombinant GST-palladin and the reactivity was blocked by preadsorption with the antigenic peptide (Figure 3A). In cell lysates, the antiserum reacted with a major band of ~95 kDa and additionally with a 140-kDa band (Figure 3B). The preimmune sera did not recognize these bands (our unpublished data), and the reactivity of palladin antibody could be blocked by preincubation with the antigenic peptide (Figure 3B). Western blot analysis of tissue lysates showed strong reactivity in prostate, ovary, and colon, tissues positive in mRNA analysis, and in kidney, whereas hematopoietic tissues expressed little palladin. Comparison of the expression of palladin and myotilin in smooth muscle (prostate) and skeletal muscle demonstrated reciprocal expression, i.e., strong expression of palladin in smooth muscle and weak expression in skeletal muscle and vice versa.

Localization of Palladin

The subcellular localization of palladin was studied by indirect immunofluorescence microscopy of cultured cells. In HISM cells, a fibrillar periodical punctate staining pattern was observed (Figures 4, A and B, and 7A). The most intense staining was detected at the filament ends. To study whether the localization was associated with the actin cytoskeleton, we double-stained the cells with FITC-labeled phalloidin for F-actin (Figure 4C). An overlay image demonstrates a colocalization of the two proteins, and implies that palladin is associated with microfilaments (Figure 4D). Staining of HISM cells with the preimmune serum did not reveal any specific reactivity (our unpublished data). Immunolocalization of palladin in U251mg (Figure 5A) and HeLa (Figure 5B) cells demonstrated a pattern that resembled that seen in HISM cells. The fibrillar punctate staining along stress fibers was most notable in cells that were well spread and relatively large.

We studied next, whether transfection of the C-terminal Ig-domain–containing region of palladin resulted in a similar localization as the endogenous protein. A myc-tagged cDNA construct was transiently transfected into HeLa cells and detected with an anti-myc mAb. The transfected protein localized along actin microfilaments in a pattern reminiscent of the endogenous protein (Figure 5C). Transfected protein was also detected in the nucleus. At present it is unclear whether the nuclear localization is caused by transient overexpression. The transfection results confirm the immunolocalization of the endogenous protein, and indicate that the Ig-domain–containing C terminus can be targeted to microfilaments.

We also analyzed the distribution of palladin in frozen sections of a human stomach carcinoma specimen (Figure 6). A strong staining was observed in the smooth muscle layer of the stomach, and the serosal vessel walls (tunica media) (Figure 6A). Reactivity was also detected in the adenocarcinoma cells invading the muscular layer (Figure 6C). Preimmune serum showed no specific staining (Figure 6, B and D).

Interaction between Palladin and Ezrin

Because palladin was found in a two-hybrid screen with the C-terminal construct of ezrin, it was of interest to study the colocalization of these two proteins in cultured cells. Ezrin has been described as a component of the actin cytoskeleton, localizing in submembraneous structures such as microvilli and lamellipodia (Vaheri *et al*., 1997; Bretscher, 1999; Tsukita and Yonemura, 1999). Thus, the previously reported subcellular distribution is rather different from palladin. We per-

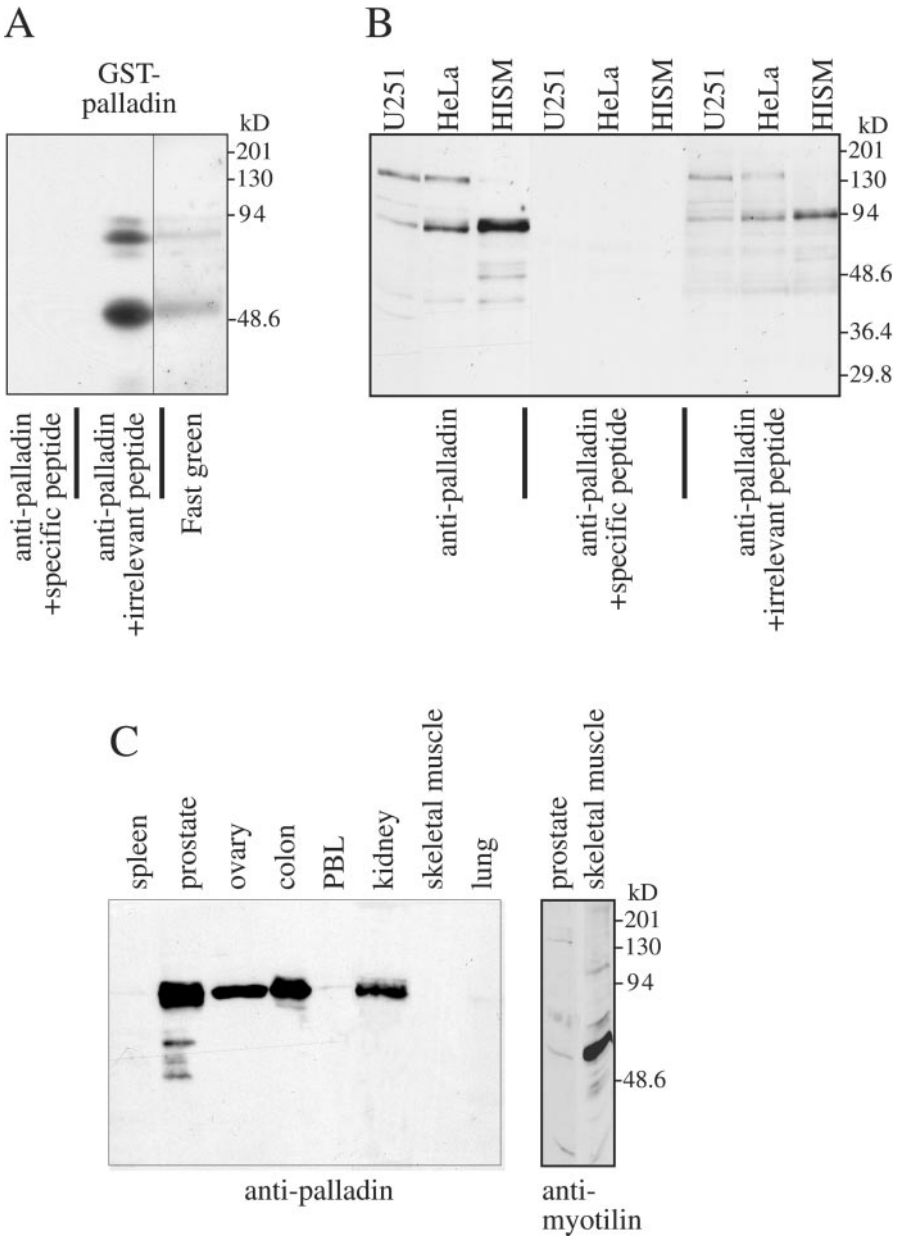

Figure 3. Western blot analysis of palladin in cell lines and tissues. (A) Recombinant GST-palladin–containing amino acids 321–772 was immunoblotted with affinity-purified palladin antibody increased against a synthetic 17-residue peptide. In addition to the 90-kDa full-length protein, a 50-kDa band apparently representing a break breakdown product is detected. The reactivity is blocked by preabsorption with 5 M excess of the antigenic peptide but not with an irrelevant peptide. The right lane shows a fast green staining of the membrane after immunoblotting. (B) Lysates from U251mg glioma cells, HeLa epidermoid carcinoma cells, and HISMs were used for immunoblotting with palladin antibody. The antibody recognizes two major polypeptide bands, a 140-kDa band in U251 and HeLa cells and a 95-kDa band in all cell types. The reactivity is blocked by preabsorption with 5 M excess of the antigenic peptide but not with an irrelevant peptide. (B) Tissue lysates were blotted with palladin antibody. A 95-kDa band is detected in several tissues. On the right, immunoblotting of prostate and skeletal muscle with myotilin antibody is shown.

formed double-staining of ezrin and palladin in several cell lines. In epithelial cells, such as HeLa, ezrin was localized at the cortical actin skeleton and demonstrated little overlap with palladin (our unpublished data). However, in HISM cells, in which another ERM protein, merlin, has previously been localized along the microfilaments (den Bakker *et al.*, 1995), the localization of ezrin was different from epithelial cells. Ezrin demonstrated a filamentous staining pattern and partial colocalization with palladin (Figure 7). This pattern was more evident if the cells were briefly detergent extracted before fixation. The subcellular localization suggests that ezrin and palladin may interact in smooth muscle cells. Because the distribution of ezrin in smooth muscle cells was unexpected, we tested by Western blotting whether structural modification of ezrin in these cells would explain the localization. The results did not reveal differences in SDS-PAGE migration of HISM cell ezrin in comparison with U251mg and HeLa cells (our unpublished data).

The regions mediating interaction between palladin and ezrin were mapped with the use of the yeast two-hybrid system (Figure 8). The two-hybrid interaction between different palladin and ezrin constructs was detected by activation of the β-galactosidase receptor gene. A C-terminal construct of ezrin (aa 278–585) interacted with palladin (Ig1–3) and with a C-terminal construct containing the second and third Ig-domains (Ig2–3), but not with a construct containing only the first Ig-domain (Ig1). Ezrin 1–585 (wt), ezrin 1–339, and ezrin 479–585 did not interact with any of the constructs.

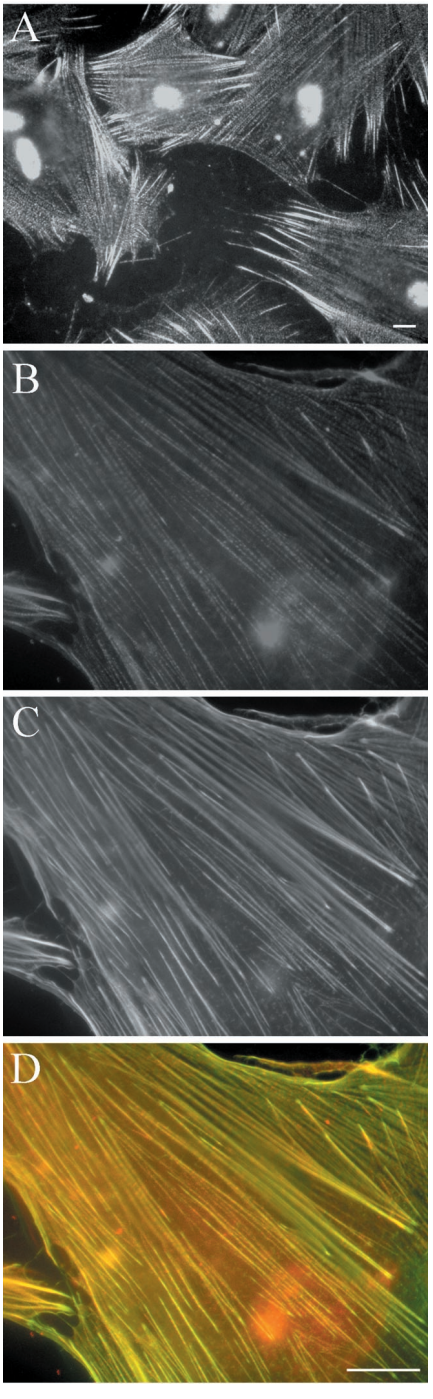

Figure 4. Localization of palladin in HISM cells. Cells were grown on to subconfluency, fixed, and stained with palladin antibody (A and B), and with FITC-phalloidin for F-actin (C). A punctate pattern of palladin can be seen along cable-like structures. The staining is strongest at the filament ends. F-actin is localized uniformly along the filaments. (D) An overlay image of B and C shows the areas of colocalization of palladin (red) and actin (green) in yellow. Bar, 5 μm.

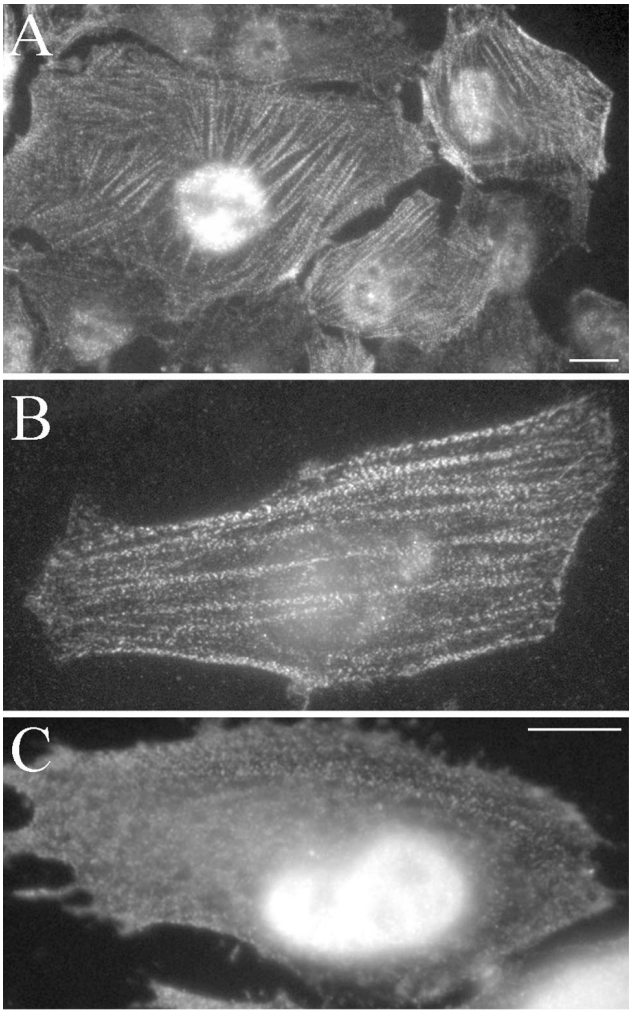

Figure 5. Localization of palladin in U251mg and HeLa cells. (A and B) Palladin was detected in U251mg (A) and HeLa (B) cells with palladin antibody as in Figure 4. Both cell types show a punctate staining pattern along actin cables. (C) HeLa cells were transiently transfected with myc-tagged palladin construct containing Ig-domains 1–3. Transfected protein, detected with anti-myc mAb, localized in the filaments in a punctate manner resembling the endogenous protein in B. In addition, nuclear staining is detected. Bar, 5 μm.

Further evidence for the interaction was obtained by additional experimental approaches. The α-helical (278–531) and C-terminal (477–585) domains of ezrin were expressed as GST-fusion proteins and bound to glutathione beads. Lysates of yeast cells expressing HA-tagged palladin Ig1, Ig2–3, and the N-terminal part of ezrin (1–309) were incubated with beads and bound proteins were detected with HA-antibody (Figure 9A). The positive control, ezrin 1–309, bound to ezrin 477–585 as described (Gary and Bretcher, 1993; Grönholm *et al.*, 1999). Palladin Ig2–3 bound to the α-helical ezrin construct but not to the C terminus, whereas palladin Ig1 bound to neither ezrin construct. The two-hybrid and affinity precipitation results indicate that the α-helical region of ezrin mediates the interaction with the C-terminal Ig-domains of palladin. The palladin binding site is apparently masked in the dormant wild-type ezrin.

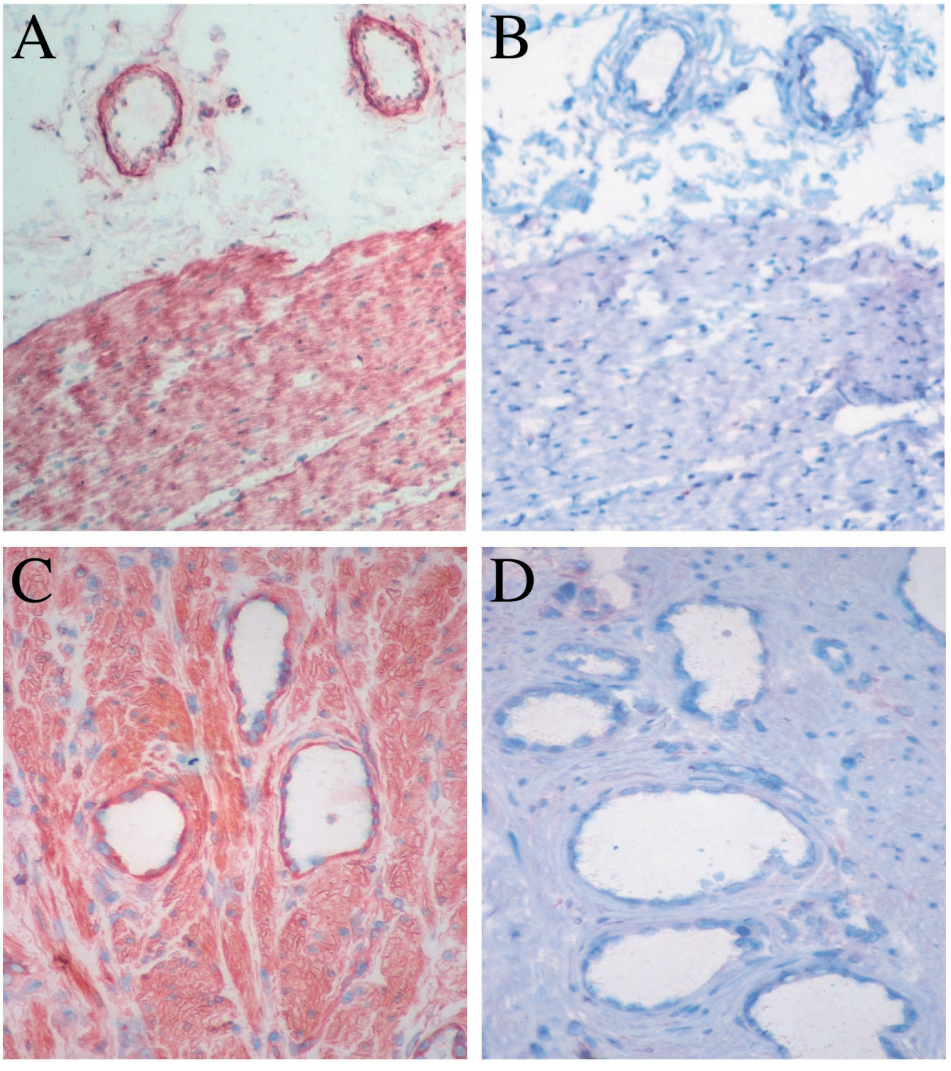

Figure 6. Immunohistochemical analysis of palladin in a stomach carcinoma specimen. Frozen sections were stained with the immunoperoxidase technique with the use of palladin antibody (A and C) or preimmune serum (B and D). Strong palladin staining is seen in the smooth muscle layer of the stomach and serosal blood vessels. In C, the invading carcinoma glands are also positive. Staining of the corresponding sections with the preimmune serum does not show specific reactivity.

The blot overlay method was used to identify whether ezrin is a major palladin-binding protein in cell lysates. Lysates of HISM and U251mg cells, full-length ezrin, and purified recombinant N-terminal half of ezrin were run in SDS-PAGE, blotted on nitrocellulose filters, and probed with biotinylated GST-palladin Ig1–3, GST-palladin Ig2–3, or GST (Figure 9B). The palladin probes bound to denatured full-length ezrin but not to the N terminus in line with the idea that the interaction site resides in the α-helical region of ezrin. In cell lysates, both probes bound to protein bands migrating at ~63 and 75 kDa and in U251mg to an additional band migrating at 85-kDa. Reprobing of the filters by ezrin antibody identified the 75-kDa as ezrin. The identity of the two other bands is not known at present.

Expression of Palladin during Dendritic Cell Differentiation

The differentiation of monocytes into dendritic cells is accompanied by drastic changes in cellular morphology. During this process, round monocytes are transformed into immature DCs containing filopodial projections and patch-like actin-containing podosomes. After further differentiation, mature DCs acquire the morphology of elongated cells with dendrite-like processes. The maturation is accompanied by up-regulation of cell surface molecules, such as CD1a in immature DCs and CD1a and CD83 in mature DCs (Figure 10A) (Zhou and Tedder, 1995; Vuckovic *et al.*, 1998). We studied the expression and localization of palladin during the maturation process. By Western blotting, peripheral blood monocytes were devoid of palladin, whereas immature and mature DCs showed an immunoreactive doublet migrating at ~95 kDa (Figure 10B). As a control, the lysates were blotted for moesin, a member of the ERM-family, which is expressed in the hematopoietic lineage. Unlike palladin, no differences were detected in the moesin expression level, although maturation-dependent post-translational modification was apparent (Figure 10B). Immunostaining demonstrated that in immature cells, palladin was concentrated into the actin-containing podosomes (Figure

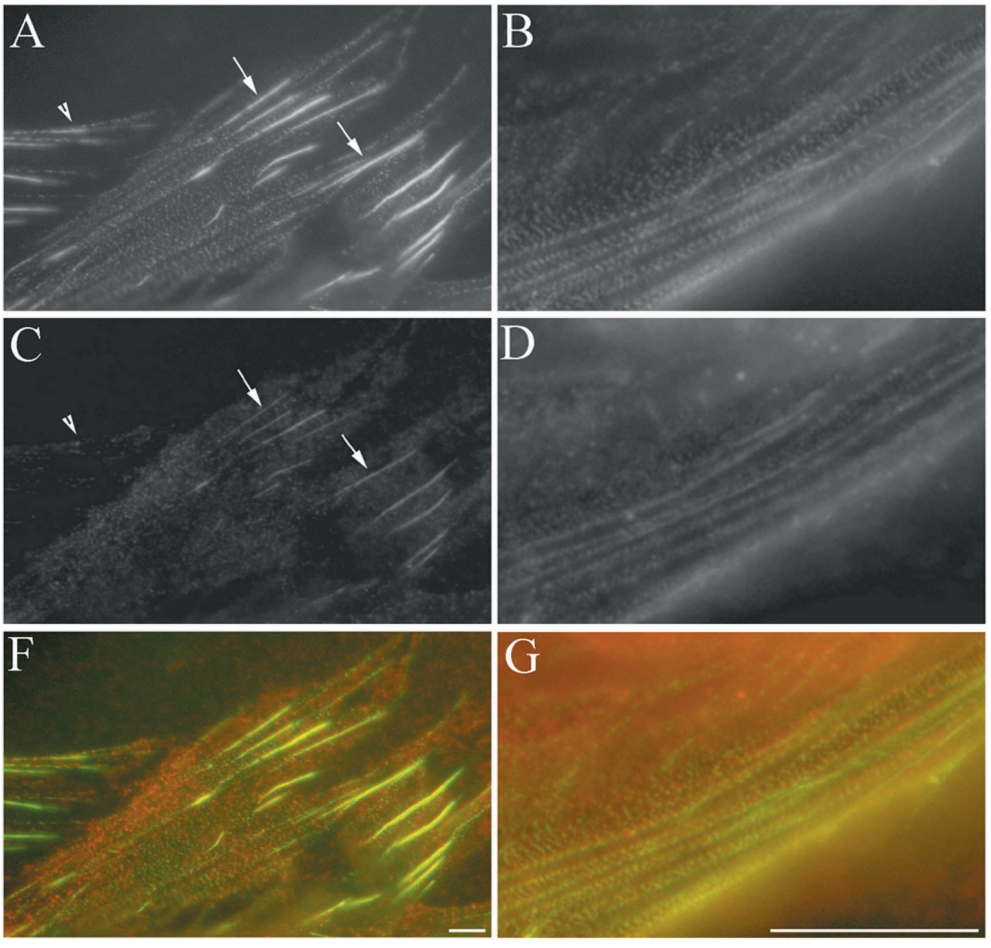

Figure 7. Localization of palladin and ezrin in HISM cells. The cells were grown on fibronectin-coated coverslips, fixed, and double-stained with palladin antibody (A and B) and with mAb 3C12 for ezrin (C and D). (A and C) At lower magnification, a colocalization of the two proteins is seen in most (arrows) but not all (arrowheads) regions abundant for palladin. (B and D) At higher magnification a punctate distribution of palladin and a more uniform ezrin staining along the same filaments is detected. (F and G) Overlay images show palladin in red, ezrin in green, and overlapping areas in yellow. Bar, 5 μm.

10C). In mature DCs, palladin decorated the thin long actin filaments (Figure 10C).

DISCUSSION

This report describes characterization of human palladin, a novel widely expressed component of the actin-containing cytoskeleton. The protein is localized along microfilaments of smooth muscle, epithelial, and glial cells in a periodic manner that is typical for the components of dense bodies of smooth muscle and dense regions in stress fibers. Human palladin and the mouse ortholog (Parast and Otey, 2000) demonstrate many similar features. Both proteins are expressed in a variety of cell types, and they are localized in a similar periodical punctate pattern along actin filaments. Both mouse and human palladin may be expressed as several isoforms, possibly dependent on the cell type. In both species, at least with the tested antibodies, the major immunoreactive bands migrate at ~95 and 140 kDa.

Palladin contains three Ig-domains and is thus a new member of a family of cytoplasmic proteins with these structural modules. All of the family members are components of the cytoskeleton and most of them associate with sarcomeric myosin. A notable exception is the actin-associated protein myotilin, which shares highest homology with palladin. The Ig-domains may provide rigidity for the proteins and function as a ruler separating structural components at a proper distance (Puius *et al*., 1998), but they also provide elasticity for the titin molecule (Linke *et al*., 1998; Trombitas *et al*., 1998; Witt *et al*., 1998). Ig-domains also serve as sites for intermolecular interactions. For instance, in myotilin the Ig-domains serve as a dimerization interface (Storbjörk, Salmikangas, and Carpén, unpublished results), the Ig-domains Z1-Z2 of titin bind to T-cap protein (Gregorio *et al*., 1998), and the Ig-domains of MyB-C interact with the A-band super-repeats of titin (Okagaki *et al*., 1993).

Palladin contains two polyproline stretches, the first of which has a consensus binding site for the EVH1 domain present in the Ena/VASP/WASP family of proteins. This FPPPP peptide sequence is found in proteins such as ActA, zyxin, and vinculin that all bind tightly to the EVH1 domain (Prehoda *et al*., 1999). The recognition of FPPPP by the EVH1 domain targets Ena/VASP/WASP family members to sites of cytoskeletal remodeling (Gertler *et al*., 1996; Symons *et al*., 1996). After correct localization, other regions of Ena/VASP/WASP proteins can bind to profilin and Arp2/3 proteins that directly promote actin polymerization. Thus, the structural characteristics suggest that palladin may be involved in the organization of the actin cytoskeleton.

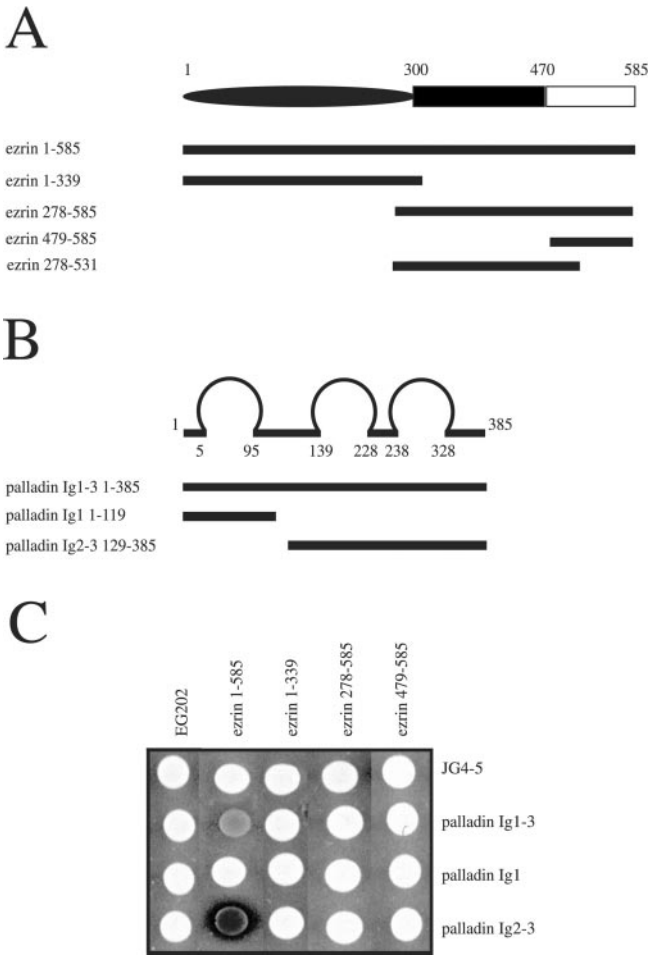

Figure 8. Yeast two-hybrid analysis of the interaction between palladin and ezrin. (A) Schematic view of ezrin and the constructs used in interaction analyses. Ezrin consists of three structural domains: N-terminal domain (black); α-helical domain (hatched box); and C-terminal domain (white box). (B) Scheme of palladin and the constructs used in interaction analyses. The loops depict Ig-domains. (C) Photomicrograph of the yeast two-hybrid interactions. On the top are marked the bait fusion proteins and on the right are the prey fusion proteins. A color reaction is an indicator of an interaction. An interaction is detected between $ezrin_{278-595}$ and palladin constructs containing Ig-domains 2 and 3. EG202, empty bait vector; JG4-5, empty prey vector.

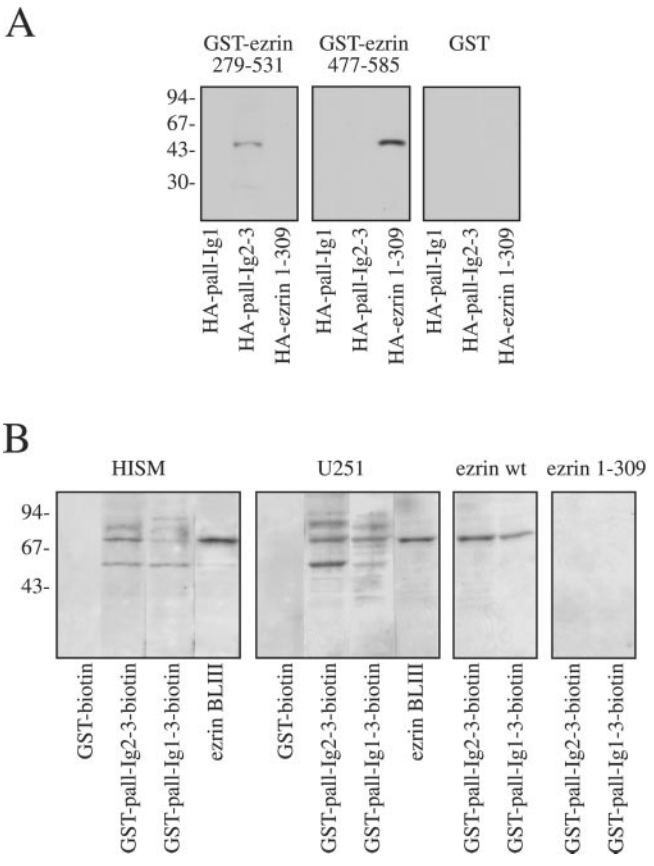

Figure 9. Affinity precipitation (A) and blot overlay (B) analysis of the interaction between palladin and ezrin. (A) Yeast lysates expressing HA-tagged palladin Ig1, Ig2–3, and ezrin 1–309 were incubated with glutathione-Sepharose–coupled GST-ezrin 279–531, GST-ezrin 477–585, and GST. After washes bound material was eluted by boiling in Laemmli sample buffer, separated by SDS-PAGE, and transferred to nitrocellulose filters. Proteins were detected by HA-immunoblotting with the use of 12CA5 mAb. Palladin Ig2–3 interacts with the α-helical domain of ezrin (279–531) but not with the C-terminal domain (477–585). As a positive control, the association of ezrin 1–309 and ezrin 477–585 is shown. (B) Total lysates of HISM and U251mg cells, purified ezrin, or recombinant ezrin 1–309 were run in SDS-PAGE and transferred to nitrocellulose filters. The filters were incubated with biotinylated probes GST, GST-palladin Ig2–3, and GST-palladin Ig1–3. Bound probe was detected with the use of HRP-conjugated extravidin and enhanced chemiluminiscence. Both palladin probes bind to two (HISM) or three (U251 mg) major protein bands. Reprobing of the blots with ezrin antibody after stripping shows that the 75-kDa band recognized by palladin is consistent with being ezrin. The probes also react with immobilized purified ezrin but not with the N-terminal domain.

Sequence comparison indicates that palladin is most homologous to myotilin. The homology is not restricted to the Ig-domains, but is extended to the N-terminal sequence. The N-terminal region, which in myotilin is responsible for interaction with α-actinin, contains sequence unique for these two molecules, and thus myotilin and palladin appear to form a subfamily within the Ig-domain–containing cytoskeletal proteins. The subcellular localization in Z-lines and an association with limb girdle muscular dystrophy 1A, a disease characterized ultrastructurally by extensive Z-line streaming, suggest a role for myotilin in the organization of actin-containing thin filaments of the sarcomere (Salmikangas *et al.*, 1999; Hauser *et al.*, 2000). It will be interesting to determine whether palladin serves an analogous function in smooth muscle and nonmuscle cells. Further functional similarity between myotilin and palladin is suggested by the fact that both myotilin and mouse palladin associate with α-actinin (Salmikangas *et al.*, 1999; Parast and Otey, 2000).

In addition to the similarities, there are notable differences between myotilin and palladin. mRNA and protein studies indicate that expression of the two proteins is differentially

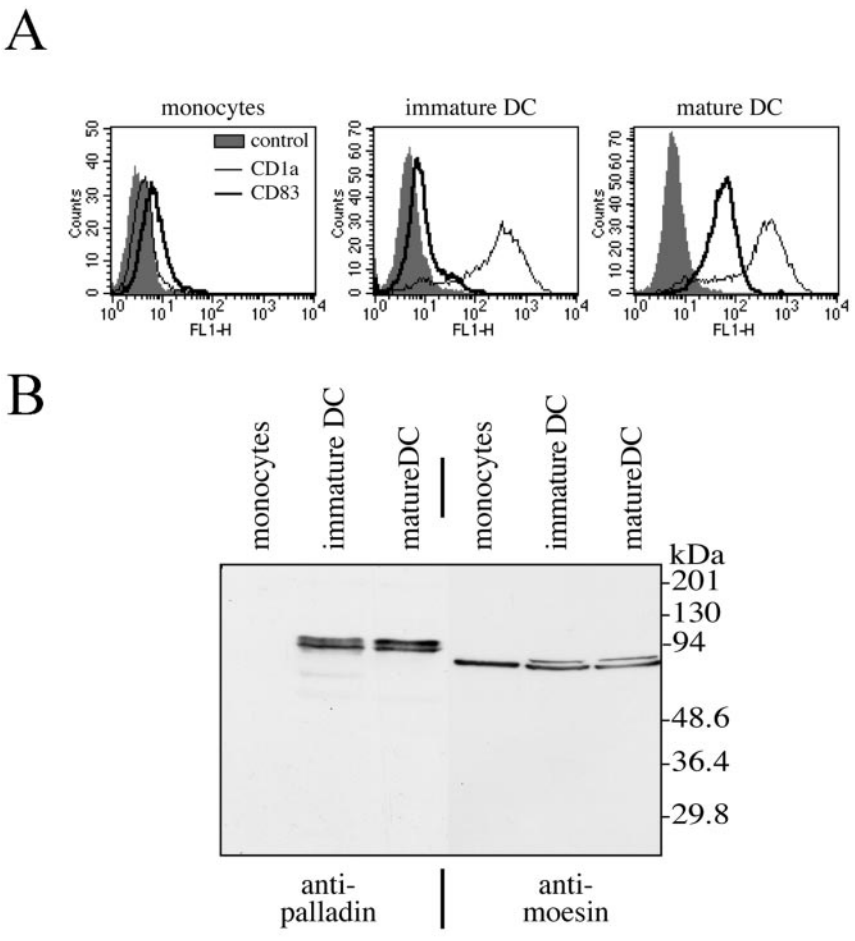

Figure 10. Expression and localization of palladin in DCs. (A) Fluorescence-activated cell sorter analysis of cell surface markers for dendritic cell differentiation (CD1a and CD83) in monocytes, immature DCs, and mature DCs. CD1a expression is up-regulated in immature dendritic cells and CD1a and CD83 expression in mature dendritic cells. (B) Western blot analysis with palladin antibody and moesin mAb in monocytes, immature DCs, and mature DCs. (C) Localization of palladin in immature DCs (left) and mature DCs (right) grown on fibronectin. In immature cells palladin is localized in patch-like podosomal structures. In mature cells, staining along the thin actin-filaments is visible. Bar, 2 μm.

regulated. The expression of myotilin in adult tissues is very restricted; it is mainly seen in striated and cardiac muscle (Salmikangas *et al.*, 1999). On the other hand, relatively strong palladin expression is seen in a variety of epithelial and mesenchymal tissues, including smooth muscle but, in comparison with myotilin, the expression level in skeletal muscle is low. This notion is also supported by the EST database information. Currently, >400 human palladin cDNAs are available. Only three of them are from skeletal muscle libraries, whereas >90% of the >40 EST myotilin cDNAs are from skeletal muscle, heart, or fetal libraries. A second difference between palladin and myotilin is that myotilin lacks the two polyproline sequences implicated in modulation of actin polymerization. This structural difference may be related to the fact that the organization of sarcomeric actin is strictly regulated, whereas in other cell types that express palladin, dynamic modulation of actin filaments by polymerization/depolymerization is a continuous process.

In vitro induced differentiation of peripheral blood monocytes into dendritic cells provides a model to study the correlation between changes in cell morphology and cytoskeletal elements. A detailed understanding of the events that control the ultrastructural alterations is still lacking, but apparently, alterations in the expression of cytoskeletal components play an important role. Previous studies have demonstrated that neoexpression of fascin, an actin bundling protein, occurs during dendritic cell differentiation (Mosialos *et al.*, 1996; Ross *et al.*, 1998). Our results show that the expression of palladin is also up-regulated during the maturation process. In immature cells, palladin is localized in podosomes, dynamic actin-containing adhesion structures that are regulated by WASP (Linder *et al.*, 1999), and in mature dendritic cells, along the delicate actin filaments. The regulated expression and subcellular localization raise the possibility that palladin is involved in the control of morphological and cytoskeletal changes associated with dendritic cell maturation. Experiments with the use of fibroblasts and Rcho-1 trophoblast cells indicate a role in cytoskeletal organization for palladin also in other cell types. In those cells, antisense treatment specifically suppresses palladin expression and concomitantly leads to disruption of stress fibers and rounding of treated cells (Parast and Otey, 2000).

Our results suggest that in palladin, Ig-domains 2–3 are responsible for the interaction with ezrin, and that they contain binding sites for at least two additional, yet unknown proteins. The fact that palladin does not interact with native full-length ezrin indicates that activation of ezrin is required for the interaction. Native ezrin molecules are in a dormant state due to intramolecular binding of the N-terminal and C-terminal association domain (Gary and Bretscher, 1993, 1995). Activation via phosphorylation and/or phosphatidylinositol bisphosphate binding disrupts the intramolecular association and unmasks binding sites for actin and several other molecules. Deletion constructs, including those used in these experiments, mimic the activated form of ezrin (Grönholm *et al.*, 1999; Mangeat *et al.*, 1999). Other characterized binding partners for ezrin include cell surface adhesion molecules, which bind to the N-terminal domain, molecules involved in cell signaling, and cytoskeletal components (Vaheri *et al.*, 1997; Bretscher, 1999; Mangeat *et al.*, 1999). The cytoskeletal components include actin, other ERM proteins, tubulin and, based on these studies, palladin. Although a variety of binding partners for ezrin has been revealed, only one of them, the RIIα subunit of protein kinase A (Dransfield *et al.*, 1997) is known to interact with the α-helical region.

The in vivo significance of the interaction between palladin and ezrin requires further studies. It is probable that the interaction occurs only in specialized cell types, such as smooth muscle cells, in which the two proteins colocalize. Palladin is associated with actin fibers in all cell types studied, whereas ezrin in epithelial, glial, and most other cell types is a component of the cortical actin cytoskeleton. Although the C-terminal constructs of ezrin and radixin have been shown to localize to stress fibers (Algrain *et al.*, 1993; Henry *et al.*, 1995), such localization has not been previously demonstrated for full-length ezrin. There are several possibilities for the unexpected localization of ezrin in smooth muscle cells. We regard major modification of ezrin as an unlikely explanation, because no differences were detected in the mobility of immunoreactive ezrin from HISM cells and other cell types. Other possibilities include the lack of relevant binding partners at the cell membrane of smooth muscle cells, differences in the signaling activity in smooth muscle and epithelial cells, which would affect the subcellular localization of ezrin, or differences in the cytoskeletal composition between smooth muscle cells and epithelial cells. Among various tissues, palladin expression is especially high in smooth muscle. It remains to be seen whether the high expression of palladin in these cells is involved in the microfilament association of ezrin.

From a functional perspective, the coexistence of palladin and ezrin in smooth muscle cytoskeleton is intriguing. Smooth muscle contractions are responsible for many vital functions of the body, including bowel movement and control of blood pressure. The contractile system is regulated by the Rho family of small GTP-binding proteins and by VASP, which coordinates the assembly of smooth muscle actomyosin filaments, and is a major target for inhibitory vasoactive agents that regulate vessel wall tension and blood pressure. Ezrin and other ERM proteins are known to function as upstream and downstream effectors of Rho activity (Matsui *et al.*, 1998; Maekawa *et al.*, 1999). Interestingly, palladin contains the FPPPP peptide consensus sequence, which serves as the binding site for EVH1 domain in Ena/VASP/WASP protein family (Prehoda *et al.*, 1999). In vascular smooth muscle cells, VASP localizes in proximity of microfilaments and dense bodies (Markert *et al.*, 1996), and it may thus interact with palladin. If such an interaction indeed takes place, the ezrin–palladin complex could bring together and coordinate two important signaling pathways, i.e., the Rho-pathway and the VASP-mediated control of the acto-myosin system.

ACKNOWLEDGMENTS

We thank Dr. T. Nagase (Kazusa DNA Research Institute, Kazusa, Japan) for providing the clone AB023209 and Dr. P. Ljungdahl (Ludwig Institute for Cancer Research, Stockholm, Sweden) for BOY1 yeast. We are also grateful to Dr. L. Heiska for invaluable help, to Drs. T. Mäkelä and M. Sainio for critical comments on the manuscript, Drs. M. Parast and C. Otey for discussions, and to T. Halmesvaara and M.-L. Mäntylä for skillful technical assistance.

This work was funded by Helsinki Biomedical Graduate School, and by grants from the Academy of Finland, Helsinki University Central Hospital, Sigrid Juselius Foundation, and the Finnish Cancer Foundation.

REFERENCES

Algrain, M., Turunen, O., Vaheri, A., Louvard, D., and Arpin, M. (1993). Ezrin contains cytoskeleton and membrane binding domains accounting for its proposed role as a membrane-cytoskeletal linker. J. Cell Biol. *120*, 129–139.

den Bakker, M.A., Tascilar, M., Riegman, P.H., Hekman, A.C., Boersma, W., Janssen, P.J., de Jong, T.A., Hendriks, W., van der Kwast, T.H., and Zwarthoff, E.C. (1995). Neurofibromatosis type 2 protein co-localizes with elements of the cytoskeleton. Am. J. Pathol. *147*, 1339–1349.

Böhling, T., Turunen, O., Jääskeläinen, J., Carpén, O., Sainio, M., Wahlström, T., Vaheri, A., and Haltia, M. (1996). Ezrin expression in stromal cells of capillary hemangioblastoma. An immunohistochemical survey of brain tumors. Am. J. Pathol. *148*, 367–373.

Bretscher, A. (1999). Regulation of cortical structure by the ezrin-radixin-moesin protein family. Curr. Opin. Cell Biol. *11*, 109–116.

Chou, R.G., Stromer, M.H., Robson, R.M., and Huiatt, T.W. (1994). Substructure of cytoplasmic dense bodies and changes in distribution of desmin and alpha-actinin in developing smooth muscle cells. Cell Motil. Cytoskeleton *29*, 204–214.

Dransfield, D.T., Bradford, A.J., Smith, J., Martin, M., Roy, C., Mangeat, P.H., and Goldenring, J.R. (1997). Ezrin is a cyclic AMP-dependent protein kinase anchoring protein. EMBO J. *16*, 35–43.

Fürst, D.O., and Gautel, M. (1995). The anatomy of a molecular giant: how the sarcomere cytoskeleton is assembled from immunoglobulin superfamily molecules. J. Mol. Cell. Cardiol. *27*, 951–959.

Gary, R., and Bretscher, A. (1993). Heterotypic and homotypic associations between ezrin and moesin, two putative membrane-cytoskeletal linking proteins. Proc. Natl. Acad. Sci. USA *90*, 10846–10850.

Gary, R., and Bretscher, A. (1995). Ezrin self-association involves binding of an N-terminal domain to a normally masked C-terminal domain that includes the F-actin binding site. Mol. Biol. Cell *6*, 1061–1075.

Geiger, B., Dutton, A.H., Tokuyasu, K.T., and Singer, S.J. (1981). Immunoelectron microscope studies of membrane-microfilament interactions: distributions of alpha-actinin, tropomyosin, and vinculin in intestinal epithelial brush border and chicken gizzard smooth muscle cells. J. Cell Biol. *91*, 614–628.

Gertler, F.B., Niebuhr, K., Reinhard, M., Wehland, J., and Soriano, P. (1996). Mena, a relative of VASP and Drosophila Enabled, is implicated in the control of microfilament dynamics. Cell *87*, 227–239.

Gregorio, C.C., et al. (1998). The NH2 terminus of titin spans the Z-disc: its interaction with a novel 19-kD ligand (T-cap) is required for sarcomeric integrity. J. Cell Biol. *143*, 1013–1027.

Grönholm, M., Sainio, M., Zhao, F., Heiska, L., Vaheri, A., and Carpén, O. (1999). Homotypic and heterotypic interaction of the neurofibromatosis 2 tumor suppressor protein merlin and the ERM protein ezrin. J. Cell Sci. *112*, 895–904.

Gyuris, J., Golemis, E., Chertkov, H., and Brent, R. (1993). Cdi1, a human G1 and S phase protein phosphatase that associates with Cdk2. Cell *75*, 791–803.

Hauser, M.A., et al. (2000) Myotilin is mutated in limb girdle muscular dystrophy 1A. Hum. Mol. Genet. *9*, 2141–2147.

Heiska, L., Alfthan, K., Grönholm, M., Vilja, P., Vaheri, A., and Carpén, O. (1998). Association of ezrin with intercellular adhesion molecules-1 and -2 (ICAM-1 and ICAM-2). Regulation by phosphatidylinositol 4,5-bisphosphate (PIP_2). J. Biol. Chem. *273*, 21893–21900.

Henry, M.D., Gonzalez-Agosti, C., and Solomon, F. (1995). Molecular dissection of radixin: distinct and interdependent functions of the amino- and carboxy-terminal domains. J. Cell Biol. *129*, 1007–1022.

Katoh, K., Kano, Y., Masuda, M., Onishi, H., and Fujiwara, K. (1998). Isolation and contraction of the stress fiber. Mol. Biol. Cell *9*, 1919–1938.

Langanger, G., de Mey, J., Moeremans, M., Daneels, G., de Brabander, M., and Small, J.V. (1984). Ultrastructural localization of alpha-actinin and filamin in cultured cells with the immunogold staining (IGS) method. J. Cell Biol. *99*, 1324–1334.

Linder, S., Nelson, D., Weiss, M., and Aepfelbacher, M. (1999). Wiskott-Aldrich syndrome protein regulates podosomes in primary human macrophages. Proc. Natl. Acad. Sci. USA *96*, 9648–9653.

Linke, W.A., Stockmeier, M.R., Ivemeyer, M., Hosser, H., and Mundel, P. (1998). Characterizing titin's I-band Ig domain region as an entropic spring. J. Cell Sci. *111*, 1567–1574.

Maekawa, M., Ishizaki, T., Boku, S., Watanabe, N., Fujita, A., Iwamatsu, A., Obinata, T., Ohashi, K., Mizuno, K., and Narumiya, S. (1999). Signaling from Rho to the actin cytoskeleton through protein kinases ROCK and LIM-kinase. Science *285*, 895–898.

Mangeat, P., Roy, C., and Martin, M. (1999). ERM proteins in cell adhesion and membrane dynamics. Trends Cell Biol. *9*, 187–192.

Markert, T., Krenn, V., Leebmann, J., and Walter, U. (1996). High expression of the focal adhesion- and microfilament-associated protein VASP in vascular smooth muscle and endothelial cells of the intact human vessel wall. Basic Res. Cardiol. *91*, 337–343.

Matsui, T., Maeda, M., Doi, Y., Yonemura, S., Amano, M., Kaibuchi, K., Tsukita, Sa., and Tsukita Sh. (1998). Rho-kinase phosphorylates COOH-terminal threonines of ezrin/radixin/moesin (ERM) proteins and regulates their head-to-tail association. J. Cell Biol. *140*, 647–657.

Mosialos, G., Birkenbach, M., Ayehunie, S., Matsumura, F., Pinkus, G.S., Kieff, E., and Langhoff, E. (1996). Circulating human dendritic cells differentially express high levels of a 55-kd actin-bundling protein. Am. J. Pathol. *148*, 593–600.

Nagase, T., Ishikawa, K., Suyama, M., Kikuno, R., Hirosawa, M., Miyajima, N., Tanaka, A., Kotani, H., Nomura, N., and Ohara, O. (1999). Prediction of the coding sequences of unidentified human genes. XIII. The complete sequences of 100 new cDNA clones from brain which code for large proteins in vitro. DNA Res. *6*, 63–70.

Niebuhr, K., Ebel, F., Frank, R., Reinhard, M., Domann, E., Carl, U.D., Walter, U., Gertler, F.B., Wehland, J., and Chakraborty, T. (1997). A novel proline-rich motif present in ActA of *Listeria* monocytogenes and cytoskeletal proteins is the ligand for the EVH1 domain, a protein module present in the Ena/VASP family. EMBO J. *16*, 5433–5444.

Okagaki, T., Weber, F.E., Fischman, D.A., Vaughan, K.T., Mikawa, T., and Reinach, F.C. (1993). The major myosin-binding domain of skeletal muscle MyBP-C (C protein) resides in the COOH-terminal, immunoglobulin C2 motif. J. Cell Biol. *123*, 619–626.

Prehoda, K.E., Lee, D.J., and Lim, W.A. (1999). Structure of the enabled/VASP homology 1 domain-peptide complex: a key component in the spatial control of actin assembly. Cell *97*, 471–480.

Parast, M.M., and Otey, C.A. (2000). Characterization of palladin, a novel protein localized to stress fibers and cell adhesions. J. Cell Biol. *150*, 643–655.

Puius, Y.A., Mahoney, N.M., and Almo, S.C. (1998). The modular structure of actin-regulatory proteins. Curr. Opin. Cell Biol. *10*, 23–34.

Romani, N., Gruner, S., Brang, D., Kampgen, E., Lenz, A., Trockenbacher, B., Konwalinka, G., Fritsch, P.O., Steinman, R.M., and Schuler, G. (1994). Proliferating dendritic cell progenitors in human blood. J. Exp. Med. *180*, 83–93.

Ross, R., Ross, X.L., Schwing, J., Langin, T., and Reske-Kunz, A.B. (1998). The actin-bundling protein fascin is involved in the formation of dendritic processes in maturing epidermal Langerhans cells. J. Immunol. *160*, 3776–3782.

Sainio, et al. (1997). Neurofibromatosis 2 tumor suppressor protein colocalizes with ezrin and CD44 and associates with actin-containing cytoskeleton. J. Cell Sci. *110*, 2249–2260.

Sallusto, F., and Lanzavecchia, A. (1994). Efficient presentation of soluble antigen by cultured human dendritic cells is maintained by granulocyte/macrophage colony-stimulating factor plus interleukin 4 and downregulated by tumor necrosis factor alpha. J. Exp. Med. *179*, 1109–1118.

Salmikangas, P., Mykkänen, O.M., Grönholm, M., Heiska, L., Kere, J., and Carpén, O. (1999). Myotilin, a novel sarcomeric protein with two Ig-like domains, is encoded by a candidate gene for limb-girdle muscular dystrophy. Hum. Mol. Genet *8*, 1329–1336.

Small, J.V., and Gimona, M. (1998). The cytoskeleton of the vertebrate smooth muscle cell. Acta Physiol. Scand. *164*, 341–348.

Stromer, M.H. (1998). The cytoskeleton in skeletal, cardiac and smooth muscle cells. Histol. Histopathol. *13*, 283–291.

Symons, M., Derry, J.M., Karlak, B., Jiang, S., Lemahieu, V., McCormick, F., Francke, U., and Abo, A. (1996). Wiskott-Aldrich syndrome protein, a novel effector for the GTPase CDC42Hs, is implicated in actin polymerization. Cell *84*, 723–734.

Trombitas, K., Greaser, M., Labeit, S., Jin, J.P., Kellermayer, M., Helmes, M., and Granzier, H. (1998). Titin extensibility in situ: entropic elasticity of permanently folded and permanently unfolded molecular segments. J. Cell Biol. *140*, 853–859.

Tsukita, Sa., and Yonemura, S. (1999). Cortical actin organization: lessons from ERM (ezrin/radixin/moesin) proteins. J. Biol. Chem. *274*, 34507–34510.

Turunen, O., Wahlstrom, T. and Vaheri, (1994). A. Ezrin has a COOH-terminal actin-binding site that is conserved in the ezrin protein family. J. Cell Biol. *126*, 1445–1453.

Vaheri, A., Carpén, O., Heiska, L., Helander, T.S., Jääskeläinen, J., Majander-Nordenswan, P., Sainio, M., Timonen, T., and Turunen, O. (1997). The ezrin protein family: membrane-cytoskeleton interactions and disease associations. Curr. Opin. Cell Biol. *9*, 659–666.

van der Ven, P., et al. (2000). Indications for a novel muscular dystrophy pathway: γ-filamin, the muscle-specific filamin isoform, interacts with myotilin. J. Cell Biol. *151*, 235–248.

Vuckovic, S., Fearnley, D.B., Mannering, S.I., Dekker, J., Whyte, L.F., and Hart, D.N. (1998). Generation of CMRF-44+ monocyte-derived dendritic cells: insights into phenotype and function. Exp. Hematol. *26*, 1255–1264.

Westermark, B., Ponten, J., and Hugosson, R. (1973). Determinants for the establishment of permanent tissue culture lines from human gliomas. Acta Pathol. Microbiol. Scand. Sect. A Pathol. *81*, 791–805.

Witt, C.C., Olivieri, N., Centner, T., Kolmerer, B., Millevoi, S., Morell, J., Labeit, D., Labeit, S., Jockusch, H., and Pastore, A. (1998). A survey of the primary structure and the interspecies conservation of I-band titin's elastic elements in vertebrates. J. Struct. Biol. *122*, 206–215.

Young, P., Ferguson, C., Banuelos, S., and Gautel, M. (1998). Molecular structure of the sarcomeric Z-disk: two types of titin interactions lead to an asymmetrical sorting of alpha-actinin. EMBO J. *17*, 1614–1624.

Zhou, L.J., and Tedder, T.F. (1995). Human blood dendritic cells selectively express CD83, a member of the immunoglobulin superfamily. J. Immunol. *154*, 3821–3835.